Proceedings of the 21st ICSMGE, Vienna, Austria, 14 – 19 June 2026. Pistrol, Adam & Schweiger (eds.)
Published by: ÖGG, Austrian Society for Geomechanics, Salzburg, Austria, ISBN 978-3-9503898-4-5
https://doi.org/10.53243/ICSMGE2026-358

Interpreting Fracture Energy in Granular Particle Crushing Using Acoustic Emission for Real-Time NDT Monitoring

Sha Luo
Mott MacDonald, Birmingham, UK, sha.luo@MottMac.com
School of Engineering, University of Birmingham, UK, s.luo@bham.ac.uk

Erdin Ibraim, Andrea Diambra
School of Civil, Aerospace and Design Engineering, University of Bristol, UK

Thomas King
Birmingham Institute for Sustainability and Climate Action, University of Birmingham, UK

Nicole Metje
School of Engineering, University of Birmingham, UK

ABSTRACT: Particle crushing is a fundamental process influencing the strength, deformation, and permeability of granular soils, with critical implications for the performance and long-term stability of underground foundations and earthwork backfills. Conventional methods for assessing particle breakage, such as particle size distribution (PSD) analysis, are inherently destructive and unsuitable for continuous or in situ monitoring. To address this limitation, this study investigated the application of acoustic emission (AE) sensing as a non-destructive technique for capturing grain crushing processes during testing by interpreting associated fracture energy under one-dimensional (1D) compression.

Laboratory experiments were conducted using single soil particles and two-dimensional chalk rod specimens subjected to controlled 1D compression. Real-time AE monitoring was employed to capture micro-mechanical fracture events, with a focus on analysing signal parameters such as cumulative AE signal strength. By correlating these AE metrics with mechanical responses and known particle breakage behaviours, a model was developed to interpret fracture energy directly from AE signal characteristics.

This approach enables a novel pathway for estimating the fracture energy during particle crushing, which can be further linked to evolving breakage indices and changes in particle size distribution. The proposed model has potential applications in real-time assessment of density changes in subsurface soils or backfills, particularly in buried infrastructure networks where invasive sampling is impractical. The findings advance the development of performance-based, non-destructive geotechnical monitoring frameworks for long-term soil stability evaluation.

KEYWORDS: Granular Materials Crushing Behaviour, One-dimensional compression, Acoustic Emission, Fracture Energy.

1 INTRODUCTION

Particle crushing is a fundamental process that governs the mechanical behaviour of granular soils, significantly influencing their strength, deformation response and permeability (Marsal, 1967; Russell, 2011). These micro-mechanical processes are particularly critical in underground foundations and backfills, where grain breakage under stress alters grading, generates fines, modifies the volume, and reshapes stress–strain behaviour (Thornton, 2000; Cheng et al., 2003; Deluzarche & Cambou, 2006). As a result, the extent and mode of particle crushing directly impact long-term stability, settlement and load-bearing capacity in geotechnical systems (Yan & Shi, 2014; Alvarez-Borges et al., 2018).

Breakage events in granular soils arise from asperity contact, grain splitting and internal fracture, and are influenced by mineralogy, porosity, particle size and shape, as well as loading conditions such as stress path, rate and saturation state (McDowell & Bolton,1998; Vulpe et al., 2014). While post-test particle size distribution (PSD) analysis is commonly used to evaluate crushing indices, this method is destructive, requires direct access to the soil and is limited to laboratory conditions (Dixon et al., 2018; Alidadi et al., 2022). As such, it is poorly suited for in situ or real-time monitoring, especially in buried or inaccessible environments.

To address these challenges, there is a growing interest for non-destructive techniques capable of detecting particle breakage in real time (Koerner, 1976, 1981; Tanimoto & Tanaka, 1986). Advanced imaging methods, such as X-ray or CT, provide detailed visualisation but are impractical for field applications due to their cost and scale limitations. In contrast, AE sensing - which detects transient stress waves generated by micro-cracking and fracture events - offers a low-cost, scalable alternative. Originally proposed by Koerner and Lord (1976) in the 1970s and 1980s, AE techniques have gained traction in recent decades for applications in soil mechanics (Smith et al., 2017; Ibraim et al., 2017; Mao et al., 2018; Luo et al., 2019).

Despite its promise, interpreting AE signal characteristics in the context of fracture energy and particle breakage remains a challenge. Most existing studies focus on AE hit count or signal amplitude but fall short of establishing quantitative links to mechanical energy dissipation during crushing. This study aims to fill this gap by developing a model that correlates AE signal parameters - including cumulative AE Signal Strength - with fracture energy associated with grain breakage under one-dimensional (1D) compression.

By integrating AE-derived fracture energy estimates with evolving breakage indices and PSD changes, this work proposes a new non-invasive framework for real-time assessment of soil or backfill particle size distribution changes. This approach offers transformative potential for performance-based geotechnical monitoring and long-term infrastructure health evaluation.

2 EXPERIMENTAL SETUP AND METHODOLOGY

This section summarises the testing methodology, focusing on the loading configuration, AE monitoring and specimen types used. Full experimental procedures, sensor calibration and detailed uncertainty analysis are available in Luo et al. (2019).

2.1 *Materials and Sample Preparation*

To capture the full mechanical spectrum of particle crushing, this study begins with single-particle tests and then progresses to two-dimensional (2D) assemblies to reflect more realistic interaction mechanisms. In the single particles (Figure 1), two types of materials were initially examined: glass beads and Himalayan rock salt. The glass beads are spherical, rigid, and low-porosity particles (SiLibeads; Specific Gravity (SG) = 2.50), tested in five diameter sizes - 1 mm, 2.5 mm, 3.5 mm, 4 mm, and 6 mm - with five particles per size. The Himalayan rock salt consists of ductile, pink-hued crystalline grains (SG = 2.17), also tested in five diameter sizes - 1 mm, 2 mm, 3 mm, 5 mm, and 6 mm - with ten particles per size. Each test was conducted twice to ensure repeatability. These particles were characterised and compressed uniaxially to assess their crushing behaviour and suitability for AE monitoring.

Building on the insights from these single-particle tests, the study introduces 2D assemblies using chalk rods to investigate more complex and collective crushing mechanisms. Chalk was selected for its well-defined fracture patterns and high acoustic sensitivity, offering a consistent and tractable medium for AE-based studies. Cylindrical rods (9 mm diameter × 9 mm height, <3% dimensional variance) were fabricated and arranged into columnar assemblies confined within rigid acrylic boundaries (Figure 2). Seven assembly types were created using 1, 2, 3, 5, and 10 columns. All assemblies except the 10-column group were tested with a single standard packing arrangement. For the 10-column samples, three packing configurations—loose, dense, and random—were used to examine how initial arrangement influences crushing behaviour. Each configuration has two samples to assess repeatability. This progressive testing - from isolated particles to structured 2D packings - forms a robust framework for evaluating AE activity across different crushing modes and provides a foundation for developing more realistic numerical models.

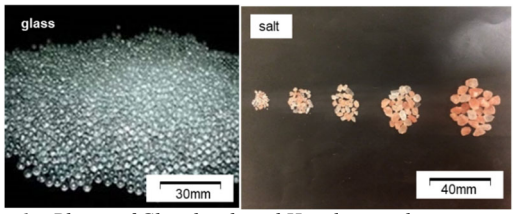

Figure 1. Photos of Glass beads and Himalayan salt.

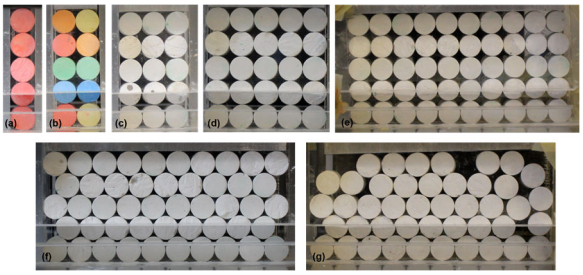

Figure 2. Side views of 2D chalk assemblies: (a) 1C, (b) 2C, (c) 3C, (d) 5C, (e) 10C-simple, (f) 10C-dense, (g) 10C-random.

2.2 *One-Dimensional Compression Setup*

All particles and chalk samples were tested under one-dimensional (1D) compression using a displacement-controlled electro-mechanical loading frame (Figure 3). The specimens were vertically compressed between two rigid steel platens: the lower one was motorised, while the upper was stationary and connected to a 5 kN reaction load cell. A Linear Variable Differential Transformer (LVDT) was employed to monitor the relative displacement between the platens. The loading rate was maintained at 0.25 mm/min, which is slow enough to avoid dynamic effects while capturing fracture progression.

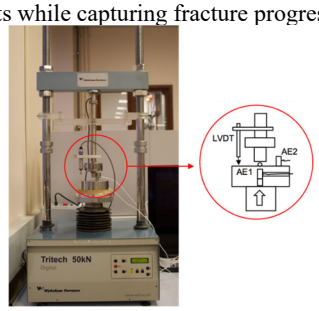

Figure 3. *Schematic of Experimental Setup*

2.3 *Acoustic Emission Sensor Setup*

Acoustic emission activity was captured using two broadband piezoelectric sensors (10 kHz–1 MHz). Both were mounted on the steel baseplate ~1 cm below the specimen using a mechanical clamp to ensure consistent coupling. Silicon grease was used as a coupling agent. AE signals were recorded in real time via a PCI-2-based acquisition system (AEWIN software, MISTRAS Group). Environmental noise testing and sensor validation were performed prior to the main test campaign. The key acquisition parameters used in the AE monitoring system are summarized in Table 1.

Table 1. AE acquisition system settings

Parameter	Value
Sample Rate (MSPS)	4
Recording Length (k)	5
Preamplifier Gain (dB)	20
Detection Threshold (dB)	36
Loading Rate (mm/min)	0.25

3 AE SIGNAL ANALYSIS AND FRACTURE ENERGY INTERPRETATION

3.1 *AE Signal Characterisation*

AE monitoring was employed to capture real-time signals associated with particle breakage and chalk rod cracking. The PCI-2-based AEWIN system (MISTRAS Group) enabled continuous tracking of transient elastic waves generated by micro-mechanical events, such as crack initiation, propagation, and crushing.

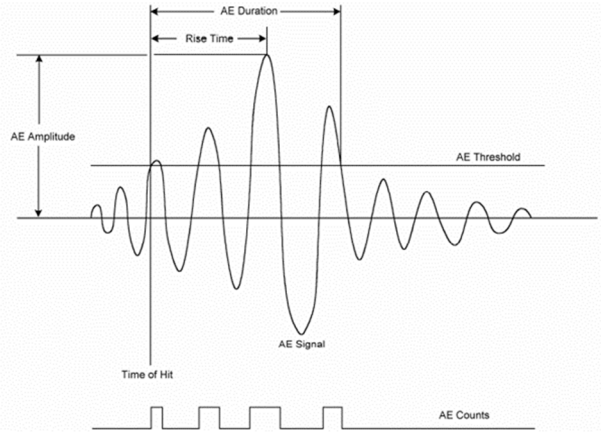

Figure 4. Schematic of AE Features *AE hits feature extraction diagram with the AE parameters definition (software AEWIN manual produced by MISTRAS company)*

The key AE features analysed include amplitude, energy, counts and duration (Figure 4). AE Signal Strength is

mathematically defined as the integral of the rectified voltage signal over the duration of the AE waveform packet, and it is calculated over the entire AE signal dynamic range and is independent of grain value, which reflects the total energy released during a discrete fracture event. Higher values generally indicate more intense cracking or splitting behaviour. The signal analysis was informed by video footage of the tests, which helped verify the correlation between visible fracture events and corresponding AE signals.

3.2 *Fracture Energy Model Development*

Fracture energy is a critical parameter in the context of granular crushing, representing the energy required to break a particle into smaller fragments. From a theoretical perspective, this energy can be linked to surface energy required to form new crack surfaces, as originally described by Griffith (1920). In this study, however, fracture energy is defined as the mechanical work exerted on a particle until its structural failure - that is, the area under the force-displacement curve (Baumgardt et al., 1975):

$$E_{fracture} = \int_0^{\Delta_c} F d\Delta \qquad (1)$$

where F is the applied compressive force, Δ is the measured displacement and Δ_c is the critical displacement at breakage. Equation (1) captures the mechanical work exerted on a particle until its structural failure.

4 RESULTS AND DISCUSSION

4.1 *Fracture Energy measured from force-displacement curves*

In this study, AE signal strength was employed as a proxy to evaluate the fracture energy released during one-dimensional compression of both granular particles and cylindrical assemblies. Among various AE parameters, signal strength exhibited the most consistent correlation with particle breakage, as confirmed by high-speed imaging and post-test image analysis. These observations confirm that AE activity aligns closely with the mechanical response of the materials. Fracture energy was also quantitatively derived from the mechanical response using Equation (1) in Section 3.2. The area under the force–time curve, multiplied by the known loading rate, yields an estimate of the energy input up to fracture. This provides a practical approach to approximating fracture energy in AE-monitored experiments.

Figures 5-7 illustrate the force-time and AE Signal Strength-time histories for three representative specimens: a glass bead, a salt particle, and a three-column chalk rod sample. In the glass bead test (Figure 5), the compression force increases up to approximately 3.5 kN until a steep drop in force is linked to a sharp AE signal peak up to $2{\cdot}10^9$ pV·s at the point of rupture, reflecting the sudden and brittle nature of failure. The results for the salt particle (Figure 6) shows a much lower particle strength with a more gradual force increase accompanied by dispersed AE bursts throughout the loading phase. This may suggest progressive micro-fracturing in a more ductile material, but it may also be the effect of a much lower signal strength values up to about 10^7 pV·s. The chalk rod assembly (Figure 7) shows a stepwise force evolution, corresponding to sequential crack events of individual rods, where there was a clear force drop, and each marked by a burst in AE signal. These consistent AE-force patterns across different material types and configurations support the reliability of AE Signal Strength for indicating fracture energy release.

4.2 *Fracture Energy Estimation from AE Parameters*

For the particle tests, the cumulative AE Signal Strength and fracture energy were averaged for each group of particles with the same diameter. Figure 8 presents the relationship between mean cumulative AE Signal Strength and the corresponding fracture energy for both glass bead and salt particle samples. The x-axis (mean fracture energy) is plotted on a logarithmic scale, while the y-axis (cumulative AE Signal Strength) remains linear to accommodate the broad dynamic range of the data. A strong positive correlation is observed for both glass and salt particles, with glass samples exhibiting significantly higher fracture energy values (up to ~819 J) and AE Signal Strength (up to $2.8{\times}10^9$ pV·s), consistent with their brittle nature and lower porosity. The linear regression fitted to the glass data yields a coefficient of determination $R^2 = 0.9964$, indicating a near-proportional relationship between fracture energy and AE response.

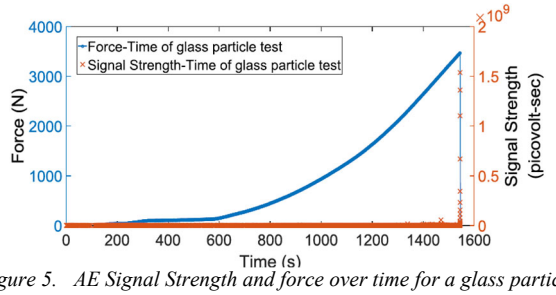

Figure 5. AE Signal Strength and force over time for a glass particle test.

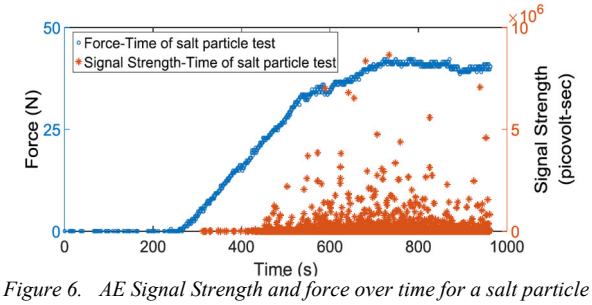

Figure 6. AE Signal Strength and force over time for a salt particle test.

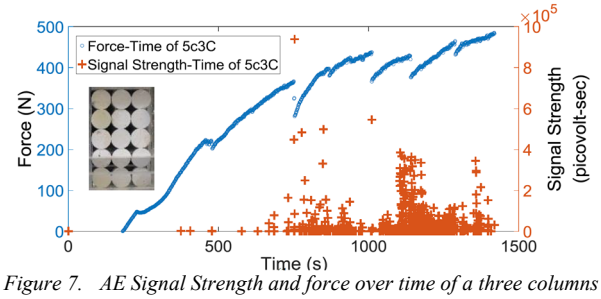

Figure 7. AE Signal Strength and force over time of a three columns chalk rode sample.

For salt samples, which are internal crystal structure, both linear and exponential fits were evaluated. The linear fit achieves a high $R^2 = 0.9612$, suggesting some degree of nonlinear AE accumulation as fracture energy increases. These trends imply that cumulative AE Signal Strength serves as a robust and material-sensitive indicator of fracture energy across particulate systems. The results highlight the potential of AE monitoring in capturing energy dissipation processes in crushable geomaterials and support its application in real-time diagnostic systems for granular fracture and compaction.

Complementary findings are shown in Figure 9, which illustrates the relationship between cumulative AE Signal Strength and corresponding fracture energy during sequential

cracking events in chalk rod specimens. The data are categorised by fracture stages - first, second, and fifth cracks - and exhibit an increasing trend in AE Signal Strength with rising fracture energy. Linear regression lines fitted to each stage illustrate strong correlations, with notably distinct behaviours at later cracking stages. These results highlight the model's sensitivity in detecting the progressive development of damage and its capability to capture the staged evolution of fracture energy throughout the failure process.

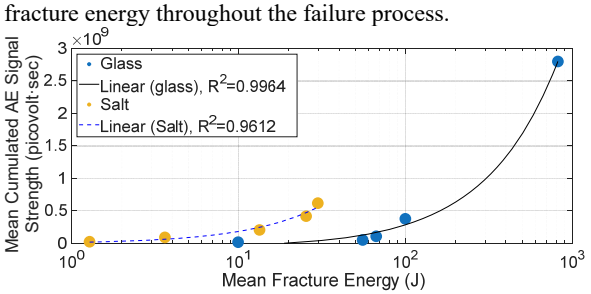

Figure 8. Mean Cumulated AE Signal Strength vs. Mean Fracture Energy in glass particles and salt particles tests

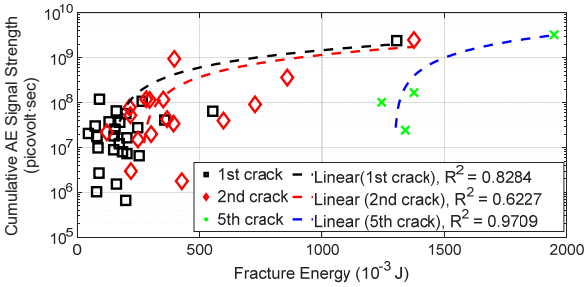

Figure 9. Cumulative AE Signal Strength vs. Fracture Energy in chalk cylinders sample tests

4.3 *Implications for Real-Time Monitoring*

Based on these observations, a semi-empirical model is proposed to estimate the fracture energy released during individual tests using AE data. The initial formulation considers only the cumulative AE Signal Strength as input, expressed as:

$$E_{fracture} = \alpha S_{cum} + \beta \qquad (2)$$

where S_{cum} is the cumulative AE Signal Strength, and α is material-specific calibration constants. The intercept β reflects pre-fracture energy accumulation not captured by AE, as well as potential signal attenuation due to sensor placement. Values of α and β are not reported here to avoid overinterpretation given the exploratory scope and limited sample size.

Since fracture energy corresponds to the energy required to generate new crack surfaces, its estimation from AE signals provides indirect insight into the evolution of internal particle fragmentation. Through established fracture mechanics principles, fracture energy can be linked to changes in crack surface area, which in turn relates to shifts in particle size distribution (PSD). As particle breakage leads to finer grading and increased surface area, this information can further be translated into bulk density changes within the granular medium. These correlations lay the groundwork for using AE-derived fracture energy as a proxy for in-situ monitoring of density evolution, compaction state, and structural stability in granular infrastructure systems.

5 CONCLUSIONS

This study demonstrated that AE sensing provides a viable, non-destructive means of estimating fracture energy during granular material crushing. By establishing a quantitative relationship between AE Signal Strength and mechanical energy dissipation, the findings support the development of real-time monitoring frameworks for particle breakage and soil density evolution. The approach holds significant promise for long-term assessment of subsurface performance in geotechnical and infrastructure systems.

6 REFERENCES

Alidadi, S., Alipour, R., Shakeri, M. 2022. Influence of rockfill particle breakage on long-term settlement of embankment dams. In: *Proceedings of the Institution of Civil Engineers-Geotechnical Engineering*, pp 1–11.

Alvarez-Borges, F. J., Madhusudhan, B. N. and Richards, D. J. 2018. The 1D normal compression line and structure permitted space of low-medium density chalk, *Géotechnique Letters 8*, No.4, 298-304.

Baumgardt, H.G., Schott, J.U., Sakamoto, Y. 1975. Shock waves and mach cones in fast nucleus-nucleus collisions. *Z Physik A* 273, 359-371.

Cheng, Y. P., Nakata, Y. and Bolton, M. D. 2003. Discrete element simulation of crushable soil, *Géotechnique* 53, No.7, 633-641.

Deluzarche, R. & Cambou., B. (2006). Discrete numerical modelling of rockfill dams. *International Journal for Numerical and Analytical Methods in Geomechanics*, *30*, 1075–1096.

Dixon, N., Smith, A., Flint, J. A., Khanna, R., Clark, B. & Andjelkovic, M. 2018. An acoustic emission landslide early warning system for communities in low-income and middle-income countries. *Landslides* 15, No. 8, 1631–1644.

Griffith, A.A. 1920. The Phenomena of Rupture and Flow in Solids. *Philosophical Transactions*: Royal Society, London, Series A, 221, 163-198.

Ibraim, E., Luo, S. & Diambra, A. 2017. Particle soil crushing: passive detection and interpretation. In *Proceedings of the 19th international conference on soil mechanics and geotechnical engineering* (eds W. Lee, J.-S. Lee, H.-K. Kim and D.-S. Kim), pp. 389–392. London, UK: International Society for Soil Mechanics and Geotechnical Engineering.

Koerner, R. M., Lord, A. E. Jr., Mccabe, W. M. & Curran, J. W. 1976. Acoustic emission behavior of granular soils. *J. Geotech. Geoenviron. Engng* 102, No. 7, 761–773.

Koerner, R. M., McCabe, W. M. & Lord, A. E. 1981. Acoustic emission behavior and monitoring of soils. In *Acoustic emissions in geotechnical engineering practice* (eds V. P. Drnevich and R. E. Gray), ASTM STP 750, pp. 93–141. West Conshohocken, PA, USA: ASTM International.

Luo, S., Ibraim, E. and Diambra, A. 2019. Acoustic emission monitoring of crushing of an analogue granular material, *Géotechnique Letters* 9, No. 4, 305-313.

Mao,W., Yang, Y., Lin,W., Aoyama, S. & Towhata, I. 2018. High frequency acoustic emissions observed during model pile penetration in sand and implications for particle breakage behavior. *Int. J. Geomech.* 18, No. 11, 04018143.

Marsal, R.J. 1967. Large Scale Testing of Rockfill Materials, *Journal of the Soil Mechanics and Foundations Division*, Vol. 93, Issue 2, pp27-43,

McDowell, G. R. and Bolton, M. D. 1998. On the micro mechanics of crushable aggregates," *Geotechnique*, Vol. 48, No. 5, pp. 667-679.

Russell, A. R. 2011. A compression line for soils with evolving particle and pore size distributions due to particle crushing, *Géotechnique Letters* 1, No. 1, 5-9.

Smith, A., Dixon, N. & Fowmes, G. 2017. Early detection of first-time slope failures using acoustic emission measurements: large-scale physical modelling. *Géotechnique* 67, No. 2, 138–152.

Tanimoto, K. & Tanaka, Y. 1986. Yielding of soil as determined by acoustic emission. *Soils Found*. 26, No. 3, 69–80.

Thornton, C. 2000. Numerical simulations of deviatoric shear deformation of granular media. *Geotechnique* 50, No.1, 43–53.

Vulpe, C., Gourvenec, S. and Power, M. 2014. A generalised failure envelope for undrained capacity of circular shallow foundations under general loading. *Géotechnique Letters* 4, No. 3, 187-196.

Yan, W. M. & Shi, Y. 2014. Evolution of grain grading and characteristics in repeatedly reconstituted assemblages subject to one-dimensional compression, *Géotechnique Letters* 4, No. 3, 223-229.